Online Journal of Earth Sciences
MEDWELL PUBLICATIONS SINCE 2000

Comparative Assessment of Analytical Models used for Aquifer Geo-Hydraulic Estimation in Imo River Basin, Nigeria

[1]T.T. Emberga, [1]A.I. Omenikolo, [2]A.I. Opara, [2]S.O. Onyekuru and [2]C.C. Agoha
[1]*Department of Physics/Electronics, Federal Polytechnic Nekede, Owerri, Nigeria*
[2]*Department of Geology, Federal University of Technology, P.M.B. 1526 Owerri, Nigeria*

Key words: Da-Zarrock parameters, geo-hydraulic, transmissivity, aquifer storativity

Corresponding Author:
T.T. Emberga
Department of Physics/Electronics, Federal Polytechnic Nekede, Owerri, Nigeria

Page No.: 1-16
Volume: 15, Issue 1, 2021
ISSN: 1991-7708
Online Journal of Earth Sciences

Abstract: Comparative Assessment of Analytical models used for Aquifer geo-hydraulic Estimation in Imo River Basin Nigeria was carried out to determine the best geophysical models in estimating the hydraulic properties of aquifer systems. The Imo River Basin lies between Latitudes 4°38'N and 6°01'N and between Longitudes 6°53'E and 7°32'E and covers an area of about 9100 km^2. The litho-stratigraphic units within the study area are Ajali Formation, Nsukka Formation, Imo Shale Formation, Ameki Formation and Benin Formation. The Da-Zarrock parameters (transverse unit resistance and longitudinal conductance) were used to determine aquifer hydraulic characteristics. A total of 569 Vertical Electrical Soundings (VES) using the ABEM terrameter (SAS) 4000 were acquired in the study area applying the Schlumberger electrode configuration and a maximum electrode spacing of 1000 m. Out of the 569 VES data points, 20 soundings (parametric soundings) were made at the vicinity of existing boreholes for comparative analysis and for quality control of the data. The hydraulic conductivity in the study area was estimated using Niwas and Singhal, Heigold model and the new geophysical model generated with an average of 13.19, 1.74 and 4.62 m/day, respectively. The study revealed a mean transmissivityT_{mean} = 140.8 m^2/day and a mean storativity of 5.3×10^{-5} for the aquiferous units in the Ajali Formation. A mean transmissivityT_{mean} = 193.5 m^2/day and mean storativity 5.54×10^{-5} were estimated in Ameki Formation. The Benin formation revealed a mean TransmissivityT_{mean} of 784 m^2/day and a mean storativity of 5.11×10^{-5}. The aquifers in the Imo Shale Formation have a mean transmissivityT_{mean} = 205.2 m^2/day with a mean storativity of 3.48×10^{-5}. The aquifers in the Nsukka Formation have a mean transmissivityT_{mean} = 211.5 m^2/day with a mean storativity of 4.8×10^{-4} while the aquifers in the Ogwasi/Asaba Formation have a mean transmissivity T_{mean} = 100.2 m^2/day with a mean storativity of 4.86×10^{-5}. The average thickness of the aquiferous units in the study area is 39.8 m while that of the aquifer depth is 115.5 m. The mean values of aquifer resistivity and aquifer conductivity are 1963.2 Ωm and 0.00186 Sm^{-1}, respectively.

INTRODUCTION

Groundwater is an essential commodity for the well-being of human societies. The quality of groundwater plays an important role in the water scarcity regions, especially for drinking water supply. During the recent decades, the groundwater exploitation has dramatically increased and hence the agricultural use of water has grown rapidly while the increasing concentration of populations in urban areas has meant that large-scale well fields have been developed for urban water supply. These situations make the groundwater more easily vulnerable to pollution.

Groundwater is a mysterious nature's hidden treasure. Its exploitation has continued to remain an important issue due to its unalloyed needs. Though there are other sources of water; streams, rivers ponds, etc., none is as hygienic as groundwater because groundwater has an excellent natural microbiological quality and generally adequate chemical quality for most uses.

For this purpose, surface geophysical methods have been used for aquifer zone delineation and evaluation of the geophysical character of the aquifer zone in several locations[1, 2].

Since, direct measurement of hydraulic conductivity is time consuming and costly, indirect methods such as predicting from readily available soil properties, e.g. particlesize distribution have been developed. Many different techniques have been proposed to determine estimate saturated hydraulic conductivity including field methods, laboratory methods and calculations from empirical formulae.

Geology and hydrogeology of the study area: The Imo River Basin lies between Latitudes 4°38'N and 6°01'N and between Longitudes 6°53'E and 7°32'E and covers an area of about 9100 km^2.

The boundaries are defined by its surface drainage divides. There are two main sub-basins within the basin: the Oramirukwa-Otamiri sub-basin and the Aba River sub-basin. The Estuary of the Imo River at the Atlantic Ocean forms the Southern boundary. There are two prominent features at North-Eastern and North-Western boundaries; these are the Udi-Okigwe-Arochukwu and the Awka-Umuchu-Umuduru sedimentary cuestas, respectively[3].

Generally, there are two different classes of formations underlying the Imo River Basin. About 80% of the basin consists in Coastal Plain Sand which is composed of non-indurated sediments represented by the Benin and Ogwashi-Asaba Formations and alluvial deposits at the estuary at the Southern end of the Imo River Basin. The remaining 20% is underlain by a series of sedimentary rock units that get younger southwestward, a direction that is parallel to the regional dip of the formations.

The Ajali Sandstone of Maastrichtian age is the oldest exposed formation in the basin, outcropping at its North-Eastern fringe along a NW-SE band (2-4 km width). It consists of thick friable, loosely consolidated sandstones[3].

Overlying the Ajali Sandstone conformably is the Nsukka Formation (Maastrichtian-Lower Paleocene) which extends to a relatively broader stretch of land than the former. It consists of alternating sequences of sandstones, shales and sandy shales. It dips at about 6°, on the average, to the south-west. The Imo Shale of Paleocene-Lower Eocene age overlies the Nsukka Formation unconformably. It consists of a thick sequence of blue and dark grey shales with occasional bands of clay-ironstones and subordinate sandstones[4].

Next in the depositional sequence is the Ameki Formation (Eocene), which consists of sand and sandstones. The lithologic units of the Ameki Formation fall into two general groups[5, 6]; an upper grey-green sandstones and sandy clay and a lower unit with fine to coarse sandstones and intercalations of calcareous shales and thin shelly limestone. Next in the depositional sequence is the Ogwashi/Asaba Formation (Oligocene to Miocene) which is generally made up of clays, sands, grits and seams of lignite alternating with gritty clay. This formation is characterized by its up dip and down dip pinch outs within the Imo Basin.

The Ogwashi/Asaba Formation is overlain by the Benin Formation (Miocene to Recent) which is the most extensive of all the formations which covers more than half of the area of the basin. It consists of sands, sandstones and gravels with intercalations of clay and sandy clay. The sands are fine-medium-coarse grained and poorly sorted. The map of the study area is shown in Fig. 1.

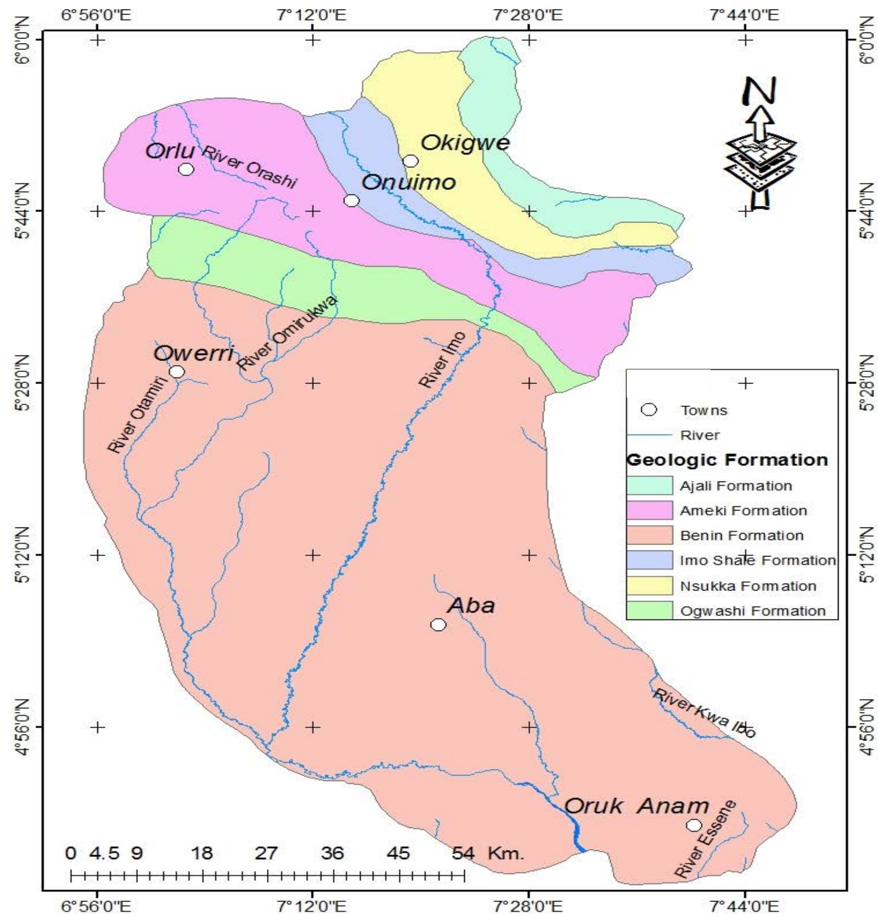

Fig. 1: Geological map of Anambra Imo River Basin[3]

MATERIALS AND METHODS

The electrical resistivity of the Earth's subsurface is mostly measured via the use of galvanic contacts. This method is based on the principle that the distribution of electrical potential in the subsurface around current-carrying electrodes depends on the electrical resistivity. The usual practice in the field is to apply an electrical direct current or low frequency alternating current between two electrodes A and B (current electrodes) implanted in the ground and to measure the potential difference between two additional electrodes M and N that do not carry current (potential electrodes). This method which is useful in groundwater study due to its ability to map the subsurface electrical resistivity structure and the interpretation helps in revealing the geologic formations and physical properties of the geologic materials.

The Schlumberger configuration was employed for resistivity data acquisition in the present study using the Abemterrameter SAS 4000. It requires the gradual separation of current electrodes in near-logarithmic manner from a fixed point at equal intervals while keeping the potential electrodes at small separations or fairly constant until acquired data becomes relatively small before increment is made[7].

The quantity measured is in reality the apparent resistivity (ρ_a), a sort of an average resistivity of the material through which the current passes owing to the fact that the earth subsurface is not necessary horizontally stratified. Using the measured current, potential difference and the geometrical setup parameters of Schlumberger array, apparent resistivity is given as follows:

$$\rho_a = \left(\frac{AB}{2}\right)^2 - \left(\frac{MN}{2}\right)^2 \times R/MN \qquad (1)$$

During the measurement, the apparent resistivity obtained from Eq. 1 is plotted as a function of AB/2 on a bi-logarithmic scale and then inverted into a resistivity model. For a single sounding, it is done in 1-D way, traditionally by assuming that the Earth is made of horizontal, homogeneous and isotropic layers with constant resistivity. The apparent resistivity curve can be inverted to estimate the resistivity and thicknesses of the layers.

The resistivity soundings were carried out at strategic locations in the study area with dense population along major roads. This pattern is adopted following the linear settlement pattern along accessible roads of the inhabitants. A total of 569 VES soundings were occupied within the study area.

The electrical resistivity contrasts existing between lithological sequences in the subsurface[8] were used in the delineation of geoelectric layers, identification of aquiferous materials and finally, the geoelectric parameters of the overburden materials was used to quantitatively evaluate the susceptibility of aquifer material.

RESULTS AND DISCUSSION

The configuration of the curve for each sounding gave an understanding on the character of the beds or layers between the surface and the maximum depth of penetration. This is because the configuration of a VES curve is a function of the number of layers in the subsurface, the thickness of each layer, and the ratio of the resistivity of the layers. Figure 2a-d shows the representative curves in the study area where as Table 1[9].

Considering the quantitative curve description, the types identified ranges from A, AH, AK, AKH, AQ, HA, H, HK, HKH, HQ, K, KA, KH, KHK, KK, KQ, Q, QH, QK, QKK , reflecting facies or lithological variations in the study area as shown in Fig. 3 and Table 1[10].

As shown in Table 1, the AK type is the most prevailing representing about 26.37% of the total curve types. This is followed by the KH-type (12.21%). The overall signature of the curves intimate and evoke alternating sequences of resistive-conductive layers.

The representative results of interpreted layer parameters from the study area is shown in Table 2 while the representation of the aquifer hydraulic parameters interpreted from the geo-electric section in the study area is presented in Table 3[11].

The aquifer hydraulic conductivity, transmissivity, storativity and hydraulic diffusivity are very useful means of confirming zones of prolific aquifers. Hydraulic conductivity refers to the ability of a material to conduct fluids under a unit hydraulic gradient[12]. This is designated by K and measured in m/day. In this study, K was estimated from the product of diagnostic constant Kσ and the aquifer apparent resistivity.

The hydraulic conductivity values estimated from Heigold model, 1979 using the formula $K_H = 386.40\ \rho^{-0.93283}$ varies from 0.0745-37.467 m/day with a mean value of 1.736 m/day as shown Table 3 and Fig. 4[13].

Table 1: Statistical representation of curve type in the study area

Curve types	Frequency	Percentage
A	49	8.672566372
AH	29	5.132743363
AK	149	26.37168142
AKH	1	0.17699115
AQ	1	0.17699115
H	39	6.902654867
HA	19	3.362831858
HH	8	1.415929204
HHQ	1	0.17699115
HK	47	8.318584071
HKH	3	0.530973451
HQ	5	0.884955752
K	23	4.07079646
KA	29	5.132743363
KH	69	12.21238938
KHK	1	0.17699115
KK	36	6.371681416
KKH	6	1.061946903
KQ	18	3.185840708
Q	8	1.415929204
QH	11	1.946902655
QK	11	1.946902655
QKK	2	0.353982301

Alternatively, the hydraulic conductivity values estimated from Niwas and Singhals, varies from 0.55-125.84 m/day with a mean value of 13.19 m/day as shown in Table 3 and Fig. 5[14].

In this study, the hydraulic conductivity values have been estimated using a new model that is Formation sensitive via the following model equations: Eq. 1 (Ajali Formation), Eq. 2 (Ameki Formation), Eq. 3 (Benin Formation), Eq. 4 (Imo Shale Formation, Eq. 5 (Nsukka Formation) and Eq. 6 (Ogwasi/Asaba), respectively as shown is shown in Fig. 4[15].

Table 4 shows aquifer conductivity and the pumping test data of Ajali Formation. The available hydraulic conductivity (pumping test) values are plotted against the aquifer conductivity where a model equation (Eq. 2) is generated. A correlation coefficient of 1 is obtained which shows a good relationship between the parameters. As shown in Eq. 2 below, the hydraulic conductivity of Ajali Formation can easily computed if the aquifer conductivity is known (Fig. 6)[16].

$$\text{Model equation for Ajali formation:}\quad K_{NM-AJ} = 8.767\sigma^{0.076} \tag{2}$$

Table 5 shows aquifer conductivity and the pumping test data of Ajali Formation. The available hydraulic conductivity (pumping test) values are plotted against the aquifer conductivity where a model equation (Eq. 3) is generated. A correlation coefficient of 0.872 is obtained which shows a good relationship between the parameters. As shown in Eq. 3 below, the hydraulic conductivity of Ameki Formation can easily computed if the aquifer conductivity is known (Fig. 7)[17].

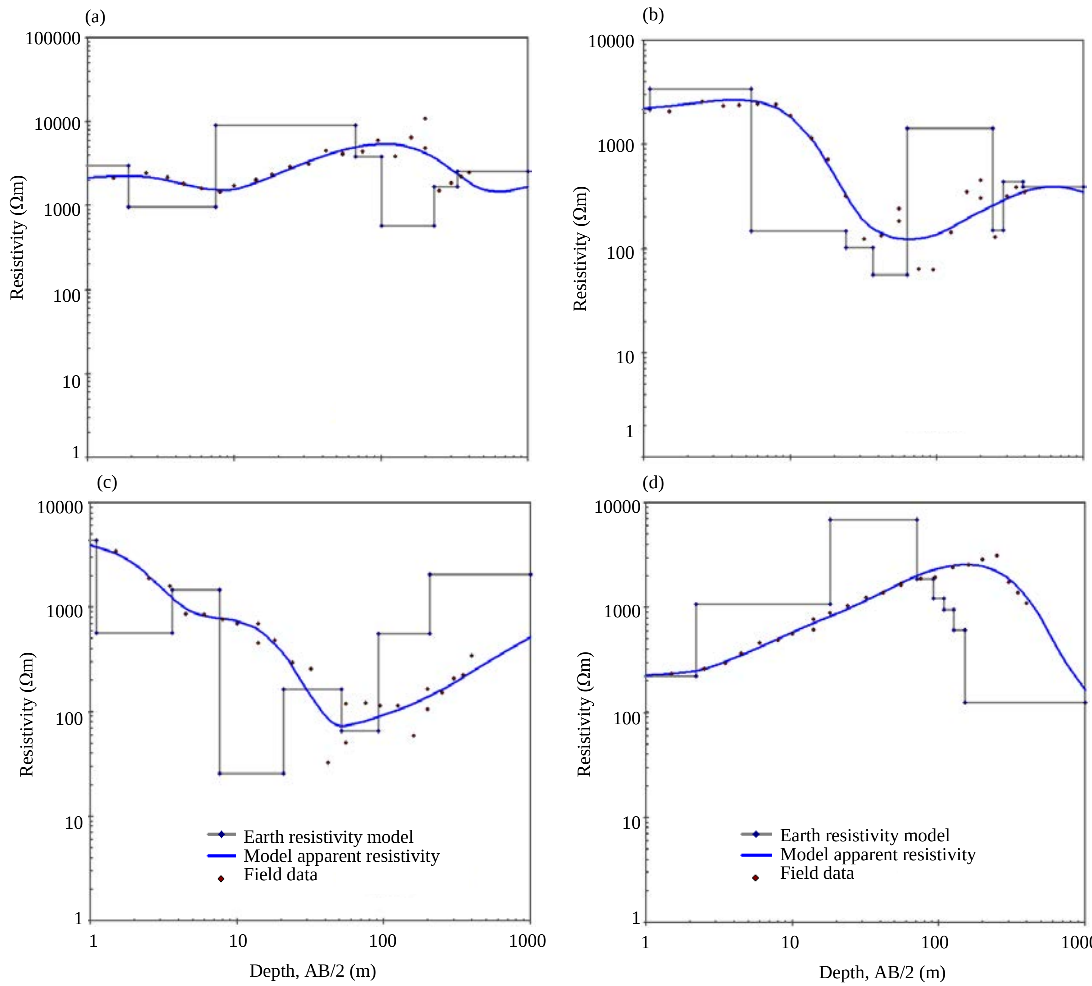

Fig. 2(a-d): Typical representative geo-electric curves generated from the resistivity data of the study area, (a) Umololo-Okigwe, (b) Ovim-Isikwuato, (c) Ubaha-Nneato and (d) Anara

Table 2: Representative results of interpreted layer parameters from the study area

VES No.	Location	No. of layers	Layer resistivity ρ (Ωm) ρ1	ρ2	ρ3	ρ4	ρ5	ρ6	ρ7	ρ8	ρ9	ρ10	Curve type
AJ 01	Obilozu IHITE-Lokpa, Umunneochi	10	133	422	82	9.2	84	388	2780	2390	2140	3540	KH
AJ 02	Eziama Lopkaukwu Umuchieze, Umunneoch	10	64.7	263	34.1	4.6	230	81	28.6	38.6	51.1	48.2	KH
AJ 03	Ubahu Nneato, Umunneochi	10	260	1030	451	8100	4790	667	667	1330	2220	3240	A
AJ 04	Nkwoagu-Amuda, Isuochi, Umunneochi	10	184	284	12.4	70	20600	13100	11900	8700	6740	5810	H
AJ 05	Eluama Lokpoukwu Umuchieze, Umunneochi	10	45.7	463	4	4.1	43.4	208	303	227	174	211	KH
AM 40	Umudimoha-Amike	5	698	450	682	6988	1345	-	-	-	-	-	A
AM 41	Umuzike, Umuoba 1	9	880	2620	###	1620	2450	4110	6590	3690	1360	-	AK
AM 42	Ogberuru	6	3510	8300	1180	840	3560	8000	-	-	-	-	H
AM 43	Onunkwo Umuele	6	598	7360	598	3060	1400	1070	-	-	-	-	AK
AM 44	Umudim Umuele Amazano	10	3860	2330	406	3020	12100	11800	1700	9200	6430	5000	A
BN 195	Umuezea-ITU	10	574	2660	1520	7200	11300	2590	2100	1970	820	696	AK
BN 196	Umuakam Eziudo	6	1030	637	2590	7320	8100	5060	-	-	-	-	H

Table 2: Continue

VES No.	Location	No. of layers	Layer resistivity ρ (Ωm) ρ1	ρ2	ρ3	ρ4	ρ5	ρ6	ρ7	ρ8	ρ9	ρ10	Curve type
BN 197	Amudi Obizi	5	3470	2120	3920	5820	311	-	-	-	-	-	Q
BN 198	Okwelle 1	8	193	4210	1040	1950	2900	1810	645	300	-	-	AK
BN 199	Okwele 2	9	193	5260	550	732	9000	3480	1890	1400	222	-	AK
IS 501	Copmp. Health Center, OSU	10	604	502	29.8	4.9	71	236	260	1250	1650	2100	H
IS 502	Umuzoho-Ezihe	8	61	186	1570	8300	2130	382	298	87	-	-	AK
IS 503	Umuduruobi Umuohiri Osuachara	10	146	3080	102	171	53.2	49.8	111	249	232	5140	KH
IS 504	Isiebu Umuduru	10	101	2640	23.5	7.4	291	69.2	29.2	23	30.2	9	KHK
IS 505	Ewuru-Umunachi	10	445	423	5	124	364	511	478	437	520	3190	H
NS 517	Obichie Ovim, Isukwuato	7	582	31400	1860	1380	686	207	13.5	-	-	-	KQ
NS 518	Umuora Agbor Umunneukwu, Isikwuato	10	165	513	1000	1190	49.1	1.8	13.4	40.1	47.8	190	KH
NS 519	Umusuh Village, Eluama, Isikwuato	9	223	3460	471	7850	1600	3540	2070	1390	860	53	KK
NS 520	Umuovo-Eluelu, Umuahia South	10	1550	9500	1010	4010	1820	860	1650	2460	2680	7620	KKH
NS 521	Oguduasa Erosion Site, Isikwuato	10	2320	688	4880	267	714	8600	34600	13700	6520	4930	HH
OG 544	Umuali 1 Mbeke (LT. COL Okejiegbe's compound)	10	1650	714	5760	340	71.2	24.1	71.8	147	220	1880	HH
OG 545	Anara	10	271	52.1	435	1180	5410	1700	679	421	305	49.3	HK
OG 546	Umuozo Ezumoha	10	295	27100	4840	632	2640	3190	4130	10900	4280	7390	KH
OG 547	Umuezeala-Umuduru	7	741	1660	2620	32200	7200	3040	733	-	-	-	AK
OG 548	Umulolo-Oboh, Osuama	8	502	4410	1030	40.8	232	1720	170	101	-	-	KH

VES No.	Location	No. of layers	Layer depth d (m) d1	d2	d3	d4	d5	d6	d7	d8	d9	Curve type
AJ 01	Obilozu Ihite-lokpa, Umunneochi	10	1.3	6.4	9.4	20	28.5	41.1	89	136	198	KH
AJ 02	Eziama Lopkaukwu Umuchieze, Umunneoch	10	0.9	3	4.4	7	19	35.4	71	115	167	KH
AJ 03	Ubahu Nneato, Umunneochi	10	0.7	8.2	19	37	59.1	81.7	106	142	172	A
AJ 04	Nkwoagu-Amuda, Isuochi, Umunneochi	10	0.9	2	7.3	17	77.6	118	114	174	235	H
AJ 05	Eluama Lokpoukwu Umuchieze, Umunneochi	10	0.6	2.4	6.3	13	21.9	46.5	89	138	186	KH
AM 40	Umudimoha-Amike	5	0.7	3	6.5	##	-	-	-	-	-	A
AM 41	Umuzike, Umuoba 1	9	0.4	8.8	17	39	60.5	88.4	138	184	-	AK
AM 42	Ogberuru	6	11	20	34	58	83.5	-	-	-	-	H
AM 43	Onunkwo Umuele	6	8.7	38	103	##	187	-	-	-	-	AK
AM 44	Umudim Umuele Amazano	10	0.5	2.9	9.9	27	66.3	102	154	204	256	A
BN 195	Umuezea-ITU	10	0.6	5.7	15	---	63.1	104	137	171	209	AK
BN 196	Umuakam Eziudo	6	9.6	19	35	61	96.4	-	-	-	-	H
BN 197	Amudi Obizi	5	13	51	60	##	-	-	-	-	-	Q
BN 198	Okwelle 1	8	0.6	3.5	10	23	44.4	60.7	79	-	-	AK
BN 199	Okwele 2	9	0.6	2.5	5	13	38.4	59.9	80	102	-	AK
IS 501	Copmp. Health Center, OSU	10	0.9	1.9	4.9	10	18.9	32	54	91	125	H
IS 502	Umuzoho-Ezihe	8	0.4	7.2	13	30	44.5	64	91	-	-	AK
IS 503	Umuduruobi Umuohiri Osuachara	10	0.4	1.9	14	36	53.9	70.6	91	114	129	KH
IS 504	Isiebu Umuduru	10	0.4	1.1	2.6	11	42.7	66.6	96	128	163	KHK
IS 505	Ewuru-Umunachi	10	0.9	7.1	21	35	55.5	80.6	105	128	156	H
NS 517	Obichie Ovim, Isukwuato	7	0.7	4.1	8.2	78	93.4	113	-	-	-	KQ
NS 518	Umuora Agbor Umunneukwu, Isikwuato	10	0.6	4.1	6	10	15.3	37	54	77	102	KH
NS 519	Umusuh Village, Eluama, Isikwuato	9	0.5	2.9	10	23	51,1	71.1	93	118	-	KK
NS 520	Umuovo-Eluelu, Umuahia South	10	0.5	1.9	7	52	79.5	125	164	204	244	KKH

Table 2: Continue

VES No.	Location	No. of layers	Layer depth d (m) d1	d2	d3	d4	d5	d6	d7	d8	d9	Curve type
NS 521	Oguduasa Erosion Site, Isikwuato	10	0.6	1.7	4.2	12	21.9	41.6	117	186	291	HH
OG 544	Umuali 1 Mbeke (LT. COL Okejiegbe's compound)	10	1	2.9	8.7	42	60.1	92	117	143	173	HH
OG 545	ANARA	10	0.8	4.5	6.8	10	29.3	44.8	61	79	99.6	HK
OG 546	Umuozo Ezumoha	10	0.4	3.1	8	33	60.1	86.4	121	179	226	KH
OG 547	Umuezeala-Umuduru	7	0.6	3.2	6.1	20	39.7	74.3	-	-	-	AK
OG 548	Umulolo-Oboh,osuama	8	0.5	2	19	42	62.1	152	243	-	-	KH

VES No.	Location	No. of layers	Layer thickness h (m) h1	h2	h3	h4	h5	h6	h7	h8	h9	Curve type
AJ 01	Obilozu Ihite-Lokpa, Umunneochi	10	1.3	5.1	3	11	8.1	12.6	48.2	48	62	KH
AJ 02	Eziama Lopkaukwu Umuchieze, Umunneoch	10	0.9	2.1	1.4	3	11.6	16.4	35.4	44	52	KH
AJ 03	Ubahu nneato, Umunneochi	10	0.7	7.5	11	18	22.4	22.6	24.3	36	30	A
AJ 04	Nkwoagu-Amuda, Isuochi, Umunneochi	10	0.9	1.1	5.3	9.6	60.7	40.4	-	60	61	H
AJ 05	Eluama Lokpoukwu Umuchieze, Umunneochi	10	0.6	1.8	3.9	6.8	8.8	24.6	42.7	49	48	KH
AM 40	Umudimoha-Amike	5	0.7	2.7	3.5	139	-	-	-	-	-	A
AM 41	Umuzike, Umuoba 1	9	0.4	8.4	8.2	22	21.5	27.9	49.6	46	-	AK
AM 42	Ogberuru	6	11	8.7	14	24	25.5	-	-	-	-	H
AM 43	Onunkwo Umuele	6	8.7	29	65	28	56	-	-	-	-	AK
AM 44	Umudim Umuele Amazano	10	0.5	2.4	7	17	36.4	38.7	52	50	52	A
BN 195	Umuezea-ITU	10	0.6	5.1	9.1	12	36.4	40.9	33	34	38	AK
BN 196	Umuakam Eziudo	6	9.6	9.2	16	26	36.3	-	-	-	-	H
BN 197	Amudi Obizi	5	13	39	38	32	-	-	-	-	-	Q
BN 198	Okwelle 1	8	0.6	2.9	6.9	13	21.5	16.3	17.9	-	-	AK
BN 199	Okwele 2	9	0.6	1.9	2.5	8	25.4	21.5	20.4	22	-	AK
IS 501	Copmp. Health Center, OSU	10	0.9	1	3	4.9	9.1	13.1	21.5	38	34	H
IS 502	Umuzoho-Ezihe	8	0.4	6.8	5.3	18	14.2	19.5	26.9	-	-	AK
IS 503	Umuduruobi Umuohiri Osuachara	10	0.4	1.5	12	22	17.9	16.7	20.6	23	15	KH
IS 504	Isiebu Umuduru	10	0.4	0.7	1.5	8	32.1	23.9	29.1	32	35	KHK
IS 505	Ewuru-Umunachi	10	0.9	6.2	14	14	20.8	25.1	24.4	23	28	H
NS 517	Obichie Ovim, Isukwuato	47	0.7	3.4	4.1	69	15.9	19.6	-	-	-	KQ
NS 518	Umuora Agbor Umunneukwu, Isikwuato	10	0.6	3.5	1.9	4.2	5.1	21.7	17.1	23	25	KH
NS 519	Umusuh Village, Eluama, Isikwuato	9	0.5	2.4	7.1	13	28.4	20.6	21.1	25		KK
NS 520	Umuovo-Eluelu, Umuahia South	10	0.5	1.4	5.1	45	27.9	45.5	39	40	40	KKH
NS 521	Oguduasa Erosion Site, Isikwuato	10	0.6	1.1	2.5	8.1	9.6	19.7	75.4	69	##	HH
OG 544	Umuali 1 Mbeke (LT. COL Okejiegbe's compound)	10	1	1.9	5.8	33	18.2	31.9	25	26	30	HH
OG 545	ANARA	10	0.8	3.7	2.3	3.5	19	15.5	16.5	18	21	HK
OG 546	Umuozo Ezumoha	10	0.4	2.7	4.9	25	26.7	26.3	34.6	58	47	KH
OG 547	Umuezeala-Umuduru	7	0.6	2.6	2.9	14	19.5	34.6	-	-	-	AK
OG 548	Umulolo-Oboh, Osuama	8	0.5	1.5	17	24	19.8	89.9	91	-	-	KH

Model equation for Ameki Formation:

$$K_{NM} -_{AM} = 21155\sigma^{1.167} \quad (3)$$

Table 6 shows aquifer conductivity and the pumping test data of Ajali Formation[18]. The available hydraulic conductivity (pumping test) values are plotted against the aquifer conductivity where a model equation (Eq. 4) is generated. A correlation coefficient of 0.914 is obtained which shows a good relationship between the parameters. As shown in Eq. 4 below, the hydraulic conductivity of Benin Formation can easily computed if the aquifer conductivity is known (Fig. 8)[19, 20].

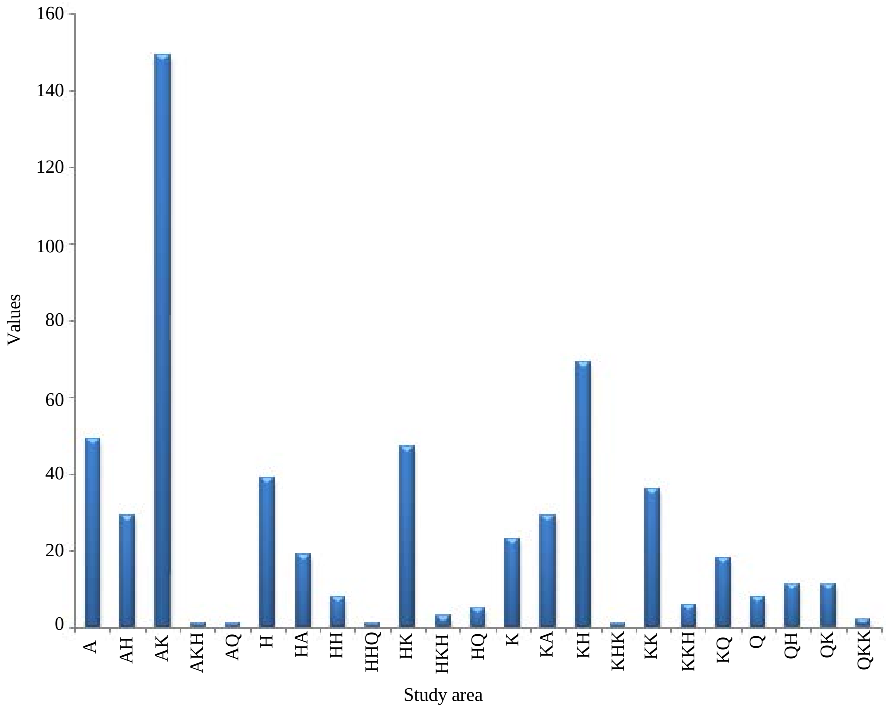

Fig. 3: Bar chart showing various curve types in the study area

Table 3: Representation of the aquifer hydraulic parameters interpreted from the geo-electric section in the study area

VES No.	Aquifer depth (m)	Aquifer Thickness h (m)	Aquifer resistivity ρ (Ωm)	Aquifer conductivity $\sigma = \rho^{-1}$ (Sm^{-1})	Transverse resistance $R = h\rho$ (Ωm^2)	Longitudinal conductance $C = h\rho^{-1}$ (Ω^{-1})	Hydraulic conductivity from pumping test K (m/day)
AJ 01	89.3	46.7	2780	0.000359712	129826	0.016798561	-
AJ 02	115	52	38.6	0.025906736	2007.2	1.347150259	-
AJ 03	142	30	1330	0.00075188	39900	0.022556391	-
AJ 04	174	61	8700	0.000114943	530700	0.007011494	-
AJ 05	89.2	48.8	303	0.00330033	14786.4	0.161056106	-
AM 40	184	46	3690	0.000271003	169740	0.012466125	-
AM 41	83.5	25.5	3560	0.000280899	90780	0.007162921	-
AM 42	187	56	1330	0.00075188	74480	0.042105263	-
AM 43	153	46	1400	0.000714286	262200	0.008070175	-
AM 44	175	50	1700	0.000588235	235000	0.010638298	-
BN 195	137	33	2100	0.00047619	69300	0.015714286	-
BN 196	35.2	16.4	2590	0.0003861	42476	0.006332046	-
BN 197	51.2	39.2	2120	0.000471698	83104	0.018490566	-
BN 198	60.7	16.3	1810	0.000552486	29503	0.009005525	4.75
BN 199	80.3	20.4	1890	0.000529101	38556	0.010793651	-
BN 200	80.4	33.9	1140	0.000877193	38646	0.029736842	-
IS 501	91	37.5	1250	0.0008	46875	0.03	-
IS 502	44.5	14.2	2130	0.000469484	30246	0.006666667	-
IS 503	91.2	20.6	111	0.009009009	2286.6	0.185585586	-
IS 504	42.7	14.1	291	0.003436426	4103.1	0.048453608	-
IS 505	80.6	25.1	511	0.001956947	12826.1	0.049119374	-
OG 544	143	26	147	0.006802721	3822	0.176870748	-

VES No.	Diagonastic constant Kσ	Average diagonastic constant Kσ (ave)	Trasmissivity T = Kh (m2/day)	Storativity $S = 1.3h/10^6$	Diffussivity $D = TS^{-1}$ (m2/day)	Hydraulic conductivity from N&S Model (K_{NSM}) $K_{NS} = K$	Hydraulic conductivity from new Model (K_{NM})	Hydraulic Conductivity from Heigold Model (K_{HM}) $KH = 386.40^{\sigma-0.93283}$
AJ 01			238.17	0.00006071	3923076.923	9.0379468	4.798479039	0.236771165
AJ 02			265.2	0.0000676	3923076.923	0.125490916	6.641564144	12.79442823
AJ 03			153	0.000039	3923076.923	4.3239098	5.07502612	0.470993151
AJ 04			311.1	0.0000793	3923076.923	28.284222	4.399947995	0.081683695

Table 3: Continue

VES No.	Diagonastic constant Kσ	Average diagonastic constant Kσ (ave)	Trasmissivity T = Kh (m2/day)	Storativity S = 1.3h/10^6	Diffussivity D = TS^{-1} (m2/day)	Hydraulic conductivity from N&S Model (K_{NSM}) $K_{NS} = K$	Hydraulic conductivity from new Model (K_{NM})	Hydraulic Conductivity from Heigold Model(K_{HM}) KH =$386.40^{-0.93283}$
AJ 05			248.88	0.00006344	3923076.923	0.98507118	5.678862675	1.871858391
AM 40			310.04	0.0000598	5184615.385	49.61158506	1.454637715	0.181805875
AM 41			171.87	0.00003315	5184615.385	47.86375144	1.516814477	0.187991415
AM 42			377.44	0.0000728	5184615.385	17.88168242	4.785636938	0.470993151
AM 43			310.04	0.0000598	5184615.385	18.8228236	4.507577425	0.121183747
AM 44			337	0.000065	5184615.385	22.8562858	3.593690914	0.145075499
BN 195			156.75	0.0000429	3653846.154	6.0739707	4.014299971	0.307589349
BN 196			77.9	0.00002132	3653846.154	7.49123053	3.488075749	0.252934866
BN 197			186.2	0.00005096	3653846.154	6.13181804	3.988886903	0.304881615
BN 198	0.002624309	0.002892367	77.425	0.00002119	3653846.154	5.23518427	4.434576023	0.353326989
BN 199			96.9	0.00002652	3653846.154	5.46657363	4.307917136	0.339355782
BN 200			161.025	0.00004407	3653846.154	3.29729838	6.044640815	0.543831758
IS 501			252.75	0.00004875	5184615.385	73.848185	7.91151708	0.499052862
IS 502			95.708	0.00001846	5184615.385	125.8373072	7.953796329	0.30354618
IS 503			138.844	0.00002678	5184615.385	6.557718828	7.722250752	4.776375736
IS 504			95.034	0.00001833	5184615.385	17.19185747	7.797037083	1.943765282
IS 505			169.174	0.00003263	5184615.385	30.18913803	7.841061837	1.149584368
OG 544			107.38	0.0000338	3176923.077	0.299096784	4.990104755	3.675348185

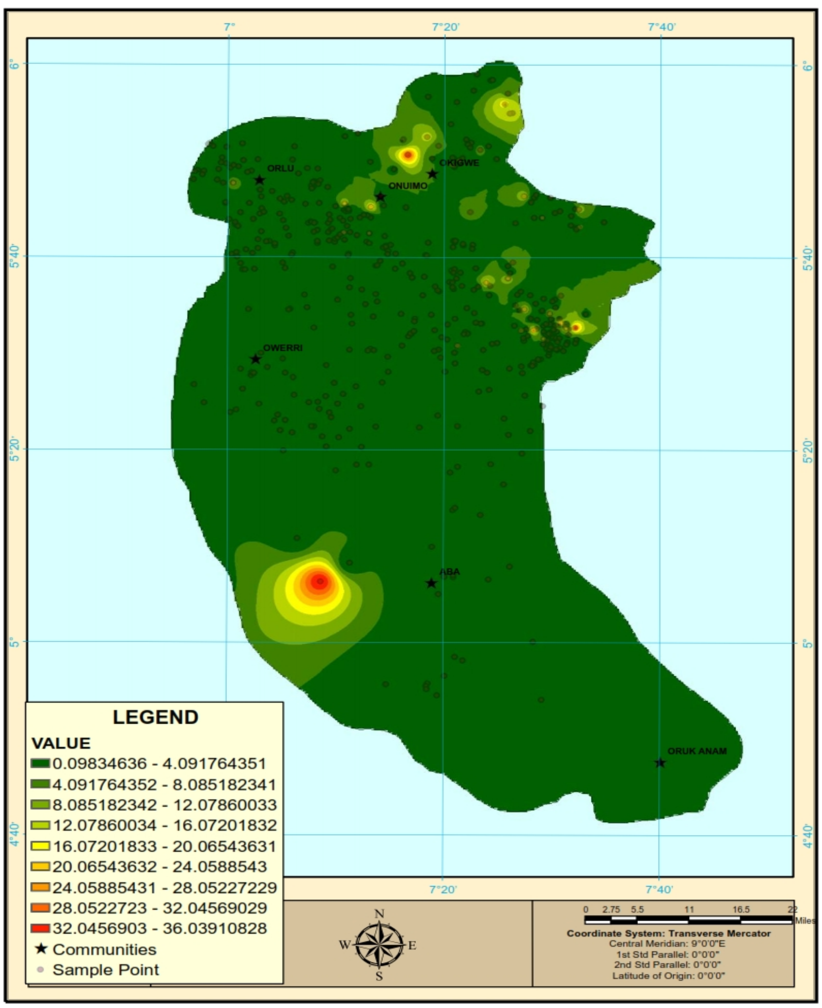

Fig. 4: Map of hydraulic conductivity estimated from Heigold[9] model in the study area

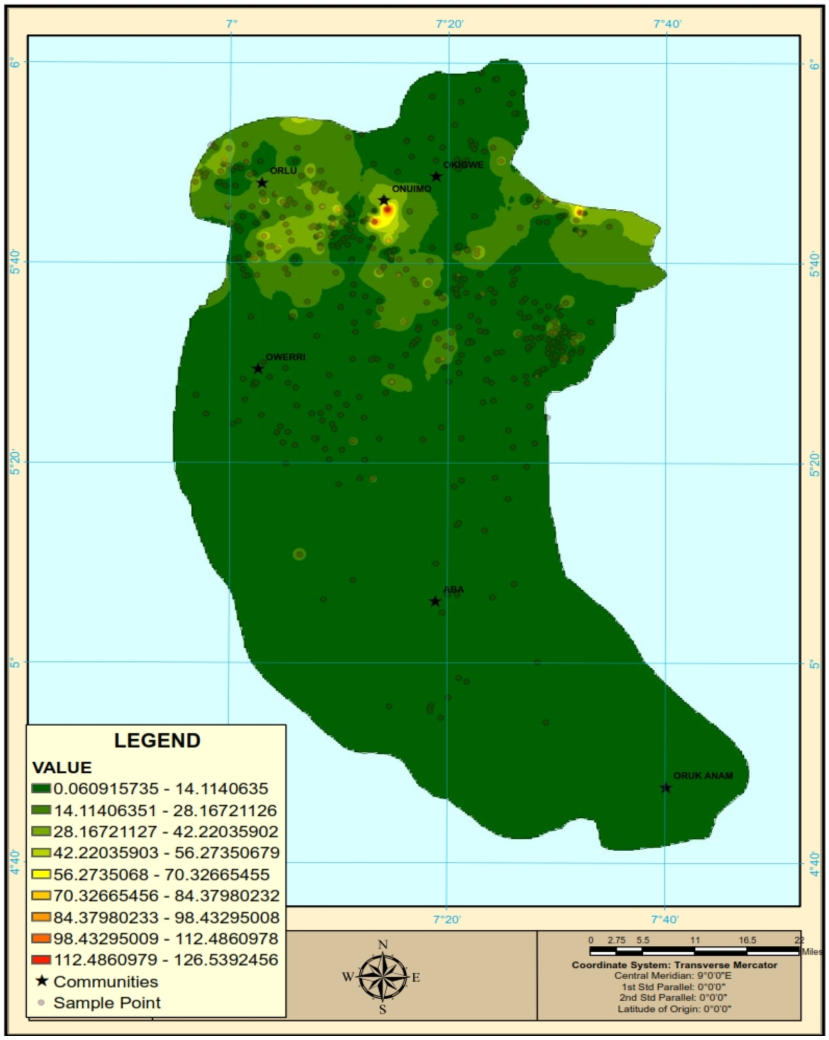

Fig. 5: Map of aquifer hydraulic conductivity estimated from Niwas and Singhals of the study area

Table 4: Ajali formation: resistivity, conductivity and pumping test values

Resistivity (Ωm)	Conductivity (Sm^{-1})	Pumping test (m/day)
1230	0.000813008	5.1
2080	0.000480769	4.9

Table 5: Ameki formation: resistivity, conductivity and pumping test values

Resistivity (Ωm)	Conductivity (S/m)	Pumping test (m/day)
1260	0.000793651	4.53
1880	0.000531915	3.2
1080	0.000819672	5.83

The model equation for Benin Formation:

$$K_{NM} -_{BN} = 675.3\sigma^{0.670} \qquad (4)$$

Table 7 shows aquifer conductivity and the pumping test data of Imo Shale Formation. The available hydraulic conductivity (pumping test) values are plotted against the aquifer conductivity where a model equation (Eq. 5) is generated[21, 22]. A correlation coefficient of 1.0 is obtained which shows a good relationship between the parameters. As shown in Eq. 5 below, the hydraulic

Table 6: Benin formation: resistivity, conductivity and pumping test values

Resistivity (Ωm)	Conductivity (S/m)	Pumping test (m/day)
1810	0.000552486	4.75
5650	0.000867257	4.9
1700	0.000588824	4.8
1180	0.000847458	6.57
1970	0.000507614	4.06
1120	0.000892857	7
6820	0.000146628	1.99
3410	0.000293255	2.39
1160	0.000862069	5.62

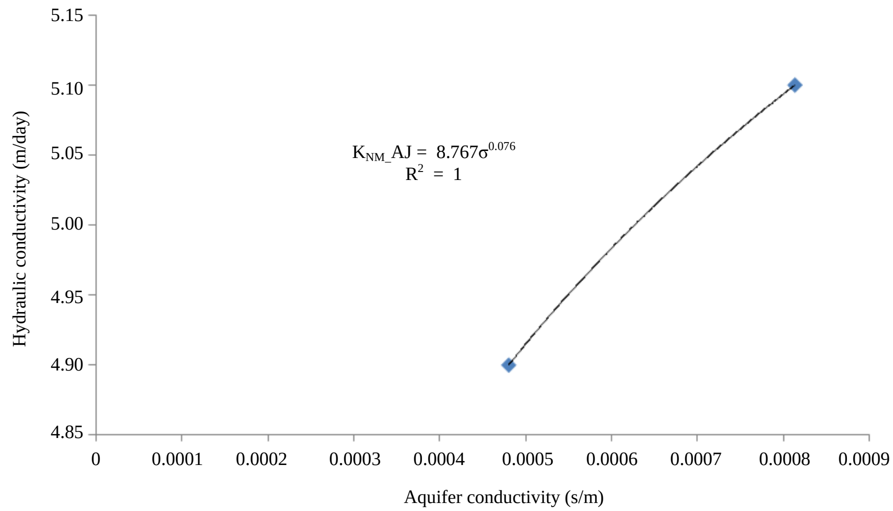

Fig. 6: A plot of aquifer hydraulic conductivity against aquifer conductivity in Ajali formation

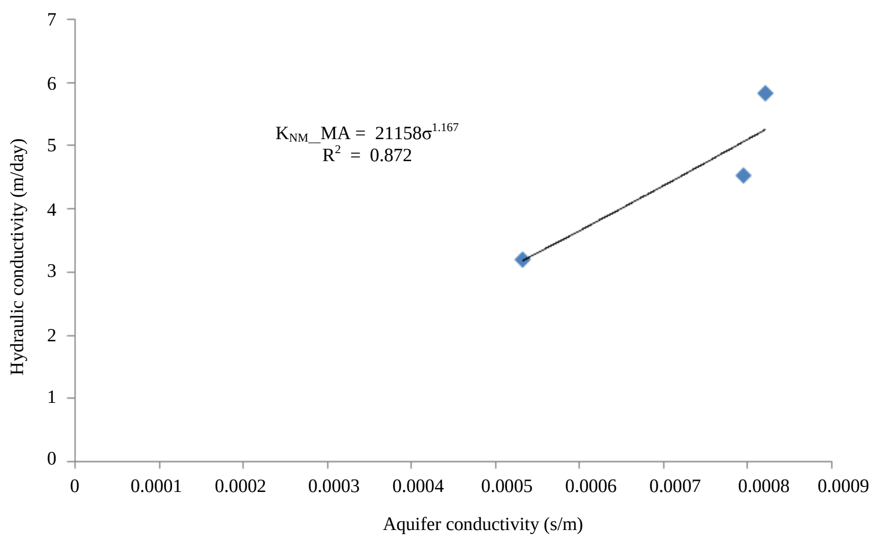

Fig. 7: A plot of aquifer hydraulic conductivity against aquifer conductivity in Ameki formation

Table 7: Imo shale formation: resistivity, conductivity and pumping test values

Resistivity (Ωm)	Conductivity (S/m)	Pumping test (m/day)
142	0.000704225	8.16
130	0.007692308	7.89

conductivity of Imo Shale Formation can easily computed if the aquifer conductivity is known in Fig. 9:

$$\text{The model equation for Imo Shale Formation:} \quad K_{NM} -_{IM} = 7.367\sigma^{0.0} \tag{5}$$

Table 8 shows aquifer conductivity and the pumping test data of Nsukka Formation. The available hydraulic conductivity (pumping test) values are plotted against the aquifer conductivity values where a model equation (Eq. 6) is generated. A correlation coefficient of 1.0 is obtained which shows a good relationship between the parameters. As shown in Eq. 6, the hydraulic conductivity of Nsukka Formation can easily computed if the aquifer conductivity is known (Fig. 10):

Table 8: Nsukka formation: resistivity, conductivity and pumping test values

Resistivity (Ωm)	Conductivity (S/m)	Pumping test (m/day)
343	0.002915494	5.01
173	0.005780347	4.13

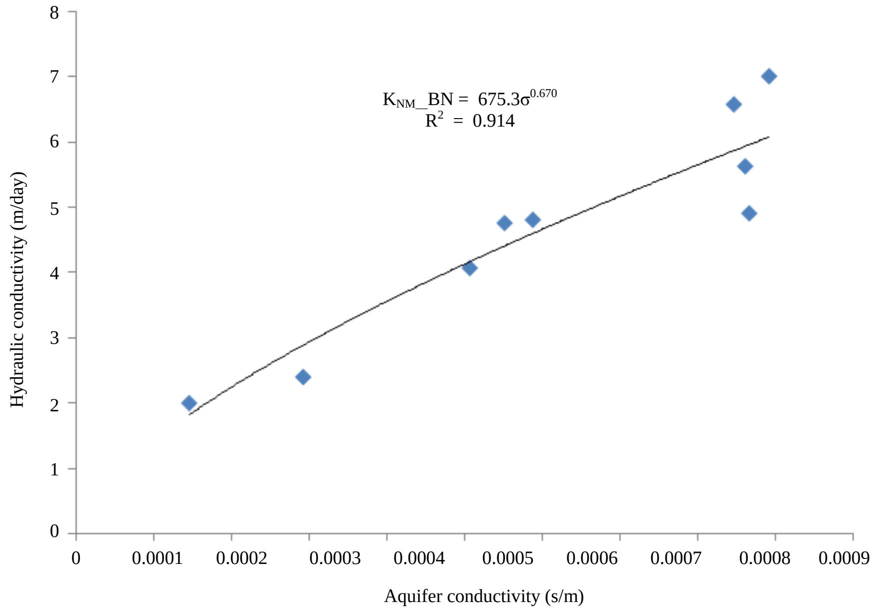

Fig. 8: A plot of aquifer hydraulic conductivity against aquifer conductivity in Benin formation

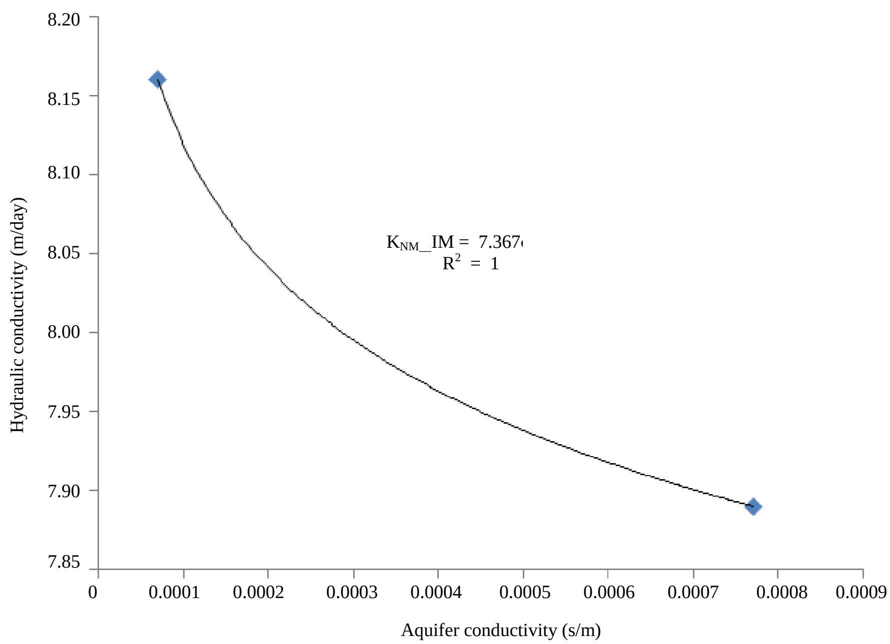

Fig. 9: A plot of aquifer hydraulic conductivity against aquifer conductivity in Imo Shale formation

The model equation for Nsukka Formation:

$$K_{NM} -_{NS} = 0.964\sigma^{0.28} \quad (6)$$

Table 9 shows aquifer conductivity and the pumping test data of Ogwasi/Asaba Formation. The available hydraulic conductivity (pumping test) values are plotted against the aquifer conductivity where a model equation (Eq. 7) is generated. A correlation coefficient of 1.0 is obtained which shows a good relationship between the

Table 9: Ogwasi/Asaba formation: resistivity, conductivity and pumping test values

Resistivity (Ωm)	Conductivity (S/m)	Pumping test (m/day)
1700	0.000588235	2.39
1040	0.000961538	2.77

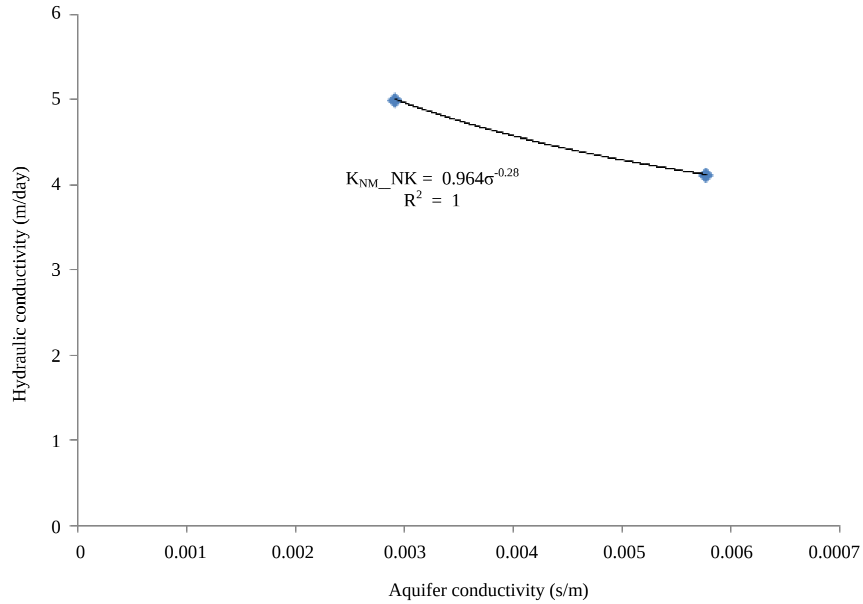

Fig. 10: A plot of aquifer hydraulic conductivity against aquifer conductivity in Nsukka formation

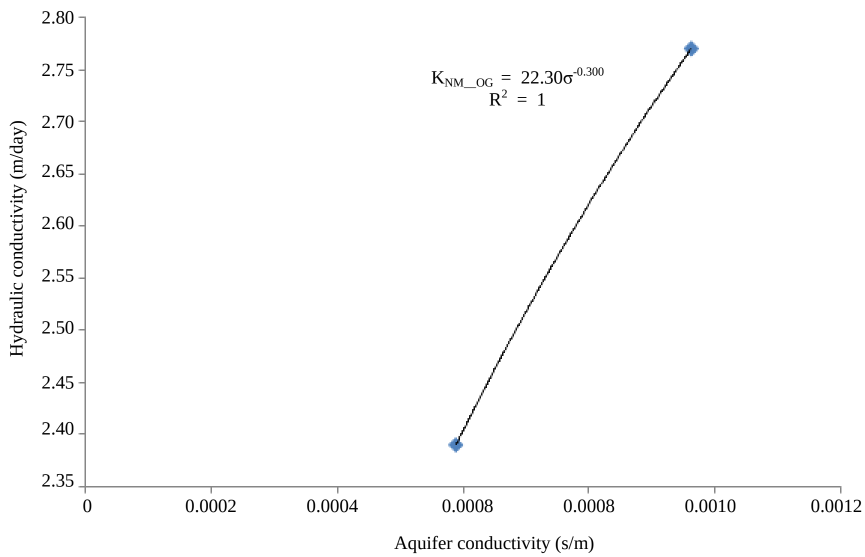

Fig. 11: A plot of Aquifer Hydraulic Conductivity against Aquifer Conductivity in Ogwasi/Asaba Formation

parameters. As shown in Eq. 7, the hydraulic conductivity of Ogwasi/Asaba Formation can easily computed if the aquifer conductivity is known (Fig. 11 and 12):

$$\text{The model equation for Ogwasi/Asaba formation:} \quad K_{NM} -_{OG} = 22.30\sigma^{0.300} \tag{7}$$

The analysis of the geo-electric curves helped in determining aquifer layer parameters which includes resistivity, depth to water table and aquifer thickness of the study area. The close agreement of the interpretation of geo-sounding data with geological information from available boreholes indicated the usefulness of the present study in characterizing aquifer geo-materials[23-25]. The vertical electrical resistivity sounding method is widely used for groundwater exploration and has been applied in many areas with a re-sounding success[26]. Despite the widespread applications, two common limitations are however associated with this technique which includes the problems of equivalence and suppression[27]. However, computer-oriented direct interpretation techniques commonly used in this study are capable of resolving

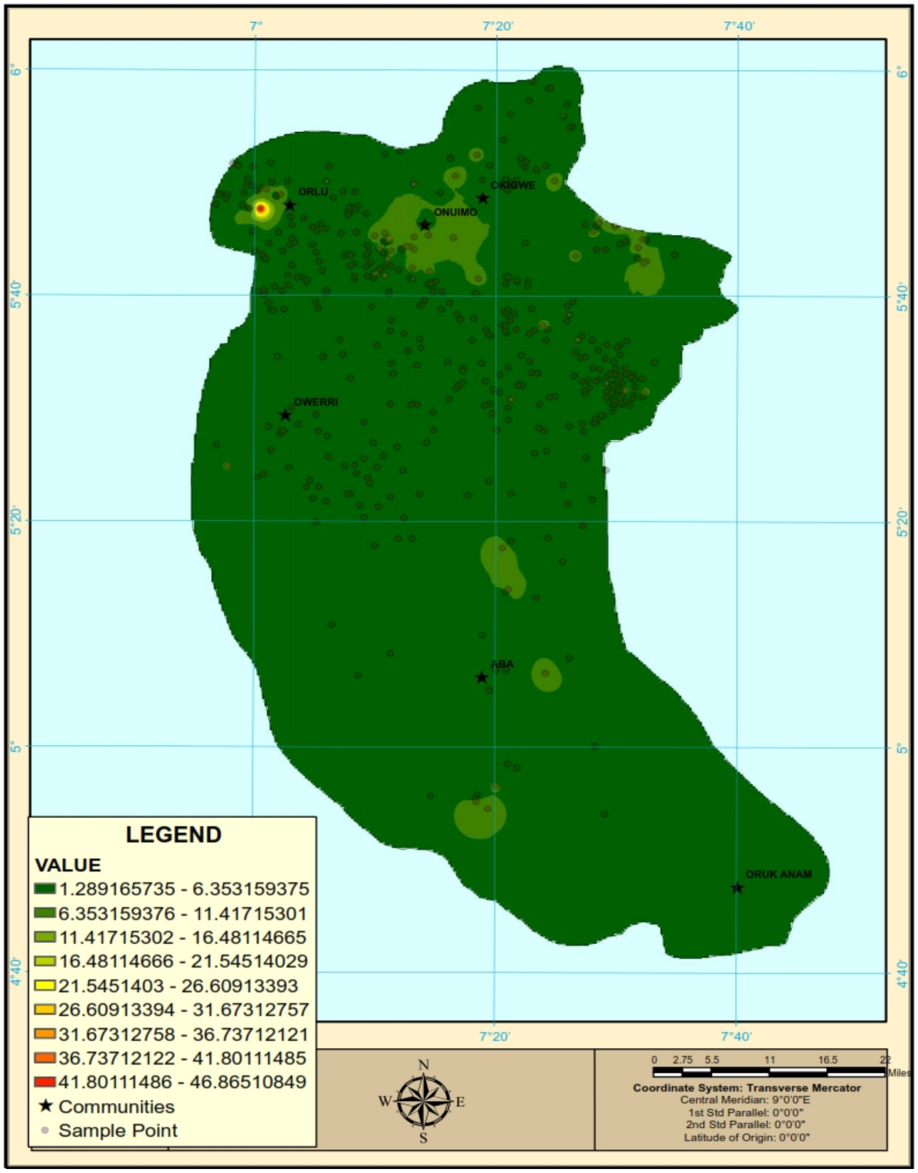

Fig. 12: Map of hydraulic conductivity estimated from new model in the study area

the thickness and resistivities of the various subsurface layers from the surface resistivity measurements. In addition, computer iterative modeling techniques are generally technically free from human bias which is always present in the conventional curve matching techniques[28].

The analysis of the aquifer electrical and geometrical parameters revealed that the aquifer resistivity ranges from 16.38-4772 m with a mean of 1963 m. The depth to the water table ranges between 10-310 m with a mean value of 89.3 m while aquifer thickness ranges from 5.7-123 m with a mean value of 47.3 m. The present study has helped to map out zones for the drilling of productive boreholes in the study area and these findings are in close agreements with earlier studies carried out in the area[3, 20].

The aquifer hydraulic conductivity in the study area estimated using Heigold[9] and the New model proposed and used in the present study gave average values of 13.19, 1.74 and 4.62 m/day, respectively. The maximum hydraulic conductivity value was recorded within the Benin Formation while the least aquifer hydraulic conductivity was recorded within the Imo Formation reported that the Benin Formation is characterized by high aquifer potentials with an estimated high aquifer hydraulic conductivity value that ranged between 5.49 and

6.63 m/day. Estimated hydraulic conductivity values in the study area are also similar to the results of earlier studies carried out close to the study area[29].

Results of the estimates of hydraulic parameters from resistivity data revealed a mean transmissivityT_{mean} = 140.8 m^2/day and a mean storativity of 5.3×10^{-5} for the aquiferous units in the Ajali Formation. A mean transmissivityT_{mean} = 193.5 m^2/day and mean storativity 5.54×10^{-5} were estimated in Ameki Formation. The Benin formation revealed a mean TransmissivityT_{mean} of 784 m^2/day and a mean storativity of 5.11×10^{-5}. The aquifers in the Imo Formation have a mean transmissivityT_{mean} = 205.2 m^2/day with a mean storativity of 3.48×10^{-5}. The aquifers in the Nsukka Formation have a mean transmissivityT_{mean} = 211.5 m^2/day with a mean storativity of 4.8×10^{-4} while the aquifers in the Ogwasi/Asaba Formation have a mean transmissivityT_{mean} = 100.2 m^2/day with a mean storativity of 4.86×10^{-5}. The highest transmissivity value was recorded within the Benin Formation while the lowest value was estimated within the Imo Shale Formation. The results of this study are similar to the findings in other studies carried out worldwide. Akhter and Hassan revealed that low values of hydraulic conductivity and transmissivity values are generally indicative of clay/shale aquifer materials while high values are generally due to the presence of sand/gravel aquifer materials. According to Ijeh and Onu, the groundwater potential in the Imo Shale Formation is low and this agrees to the low aquifer hydraulic conductivity and transmissivity values revealed by the result of the present study. The typical storativity of a confined aquifer which most often generally varies with specific storage and aquifer thickness ranges from 5×10^{-5}-5×10^{-3}[21]. The results of the present study are in agreement with the findings of Ugada *et al*.[20] carried out in the upper part of the Imo River Basin.

CONCLUSION

The estimated aquifer parameters revealed aquifer thickness and depth to water table varying from 16.7-263 m and 7.1-119 m, respectively with an average value of 39.8 m for aquifer thickness and 115.5 m for depth to water table. The resistivity of the aquiferous zones within the study area varied from 13.5-8700 Ωm with an average resistivity value of 1963 Ωm. Adopting an average transmissivity of 504.4 m^2/day, determined from pumping test, a mean hydraulic conductivity value of 7.73 m/day was obtained for the area. Hydraulic conductivity (K) values were determined using Heigold[9] and the new model generated from geophysical approach in this study. Hydraulic conductivity values using Niwas and Singhal varied from 0.55- 125. 8 m/day. The hydraulic conductivity values obtained using Heigold *et al*.[9] varied from 0.0745-37.5 m/day and those from the new model varied from 1.4-47.2 m/day. Comparison of the estimates of hydraulic conductivity obtained through the different methods, i.e., Heigold *et al*.[9] and generated new model as shown the new model values are very similar to the existing pumping test data. The hydraulic conductivity in the study area reveals an average of 13.19, 1.74 and 4.62 m/day, respectively.

ACKNOWLEDGMENT

Our profound gratitude goes the Management of Tertiary Education Trust Fund (TETFund), Nigeria year 2013-2014 (Merged) Research project Intervention for sponsoring this research work 100% through the Management of Federal Polytechnic Nekede Owerri, Nigeria. We also appreciate Management and staff of Anambra Imo River Basin Authority Nigeria for their cooperation and support during VES data acquisition.

REFERENCES

01. Babiker, I.S., M.A. Mohamed, T. Hiyama and K. Kato, 2005. A GIS-based DRASTIC model for assessing aquifer vulnerability in Kakamigahara Heights, Gifu Prefecture, central Japan. Sci. Total Environ., 345: 127-140.
02. Albinet, M. and I. Margat, 1970. [Mapping of the vulnerability to pollution of groundwater in Orleans, France (In French)]. Bull BRGM 2eme Ser., 4: 13-22.
03. Uma, K.O., 1989. An appraisal of the groundwater resources of the Imo River Basin. Nig. J. Min. Geol., 25: 305-315.
04. Engel, B., K. Navulur, B. Cooper and L. Hahn, 1996. Estimating groundwater vulnerability to nonpoint source pollution from nitrates and pesticides on a regional scale. Int. Assoc. Hydrol. Sci. Publ., 235: 521-526.
05. Aller, L., T. Bennett, J.H. Lehr, R.J. Perry and G. Hackett, 1987. Drastic: A standardized system for evaluating ground water pollution potential using hydrogeologic settings. Environmental Research Laboratory, U.S. Environmental Protection Agency Report EPA/600/2-87/035, USA.
06. Aller, L., 1985. Drastic: A standardized system for evaluating ground water pollution potential using hydrogeologic settings. Environmental Research Laboratory, Ada, Oklahoma.
07. Allen, J.R.L., 1965. Late quaternary Niger delta and adjacent areas: Sedimentary environments and lithofacies. AAPG Bull., 49: 547-600.
08. Omosuyi, G.O., J.S. Ojo and M.O. Olorunfemi, 2008. Geoelectric sounding to delineate shallow aquifers in the coastal plain sands of Okitipupa area, Southwestern Nigeria. Pac. J. Sci. Technol., 9: 562-577.

09. Heigold, P.C., R.H. Gilkeson, K. Cartwright and P.C. Reed, 1979. Aquifer transmissivity from surficial electrical methods. Groundwater, 17: 338-345.
10. Patra, H.P. and P.K. Bhattacharya, 1996. Geophysical exploration for ground water around Digha in the coastal region of West Bengal, India. Geoexploration, 4: 209-218.
11. Tesoriero, A.J., E.L. Inkpen and F.D. Voss, 1998. Assessing ground-water vulnerability using logistic regression. Proceedings of the Source Water Assessment and Protection 98 Conference, April 1998, Dallas, Texas, pp: 157-165.
12. Stempvoort, D.V., L. Ewert and L. Wassenaar, 1993. Aquifer vulnerability index: A GIS-compatible method for groundwater vulnerability mapping. Can. Water Resour. J., 18: 25-37.
13. Thapinta, A. and P.F. Hudak, 2003. Use of geographic information systems for assessing groundwater pollution potential by pesticides in Central Thailand. Environ. Int., 29: 87-93.
14. Dixon, B., 2005. Groundwater vulnerability mapping: A GIS and fuzzy rule based integrated tool. Applied Geogr., 25: 327-347.
15. Hearne, G.M., A. Wireman, S. Campbell, A. Turner and G.P. Ingersall, 1992. Vulnerability of the uppermost groundwater to contamination in the Greater Denver area, Colorado. USGS Water-Resources Investigations Report, Colorado Department of Health, Colorado.
16. Ibe, K.M. and S.C. Uzoukwu, 2001. An appraisal of subsurface geology and groundwater resources of Owerri and environs based on electrical resistivity survey and borehole data evaluation. Environ. Monit. Assess., 70: 303-321.
17. Ibe, K.M., G.I. Nwankwor and S.O. Onyekuru, 2001. Assessment of ground water vulnerability and its application to the development of protection strategy for the water supply aquifer in Owerri, Southeastern Nigeria. Environ. Monit. Assess., 67: 323-360.
18. Kalinski, R.J., W.E. Kelly, I. Bogardi, R.L. Ehrman and P.D. Yaniamoto, 1994. Correlation between DRASTIC vulnerabilities and incidents of VOC contamination of municipal wells in Nebraska. Groundwater, 32: 31-34.
19. Lobo-Ferreira, J.P. and M.M. Oliveira, 1997. DRASTIC groundwater vulnerability mapping of Portugal, groundwater: An endangered resource. Proceedings of the 27th Congress of the International Association for Hydraulic Research, August 10-15, 1997, American Society of Civil Engineers, San Francisco USA., pp: 132-137.
20. Ugada, U., K.K. Ibe, C.Z. Akaolisa and A.I. Opara, 2014. Hydrogeophysical evaluation of aquifer hydraulic characteristics using surface geophysical data: A case study of Umuahia and Environs, Southeastern Nigeria. Arabian J. Geosci., 7: 5397-5408.
21. Todd, D.K., 1980. Groundwater Hydrology. John Wiley and Sons Inc., New York, USA.,.
22. Rahman, A., 2008. A GIS based DRASTIC model for assessing groundwater vulnerability in shallow aquifer in Aligarh, India. Applied Geogr., 28: 32-53.
23. USEPA., 1985. DRASTIC: A standard system for evaluating groundwater potential using hydrogeology settings. United States Environmental Protection Agency, Ada, Oklahoma.
24. Ukandu, J.S., G.J. Udom and H.O. Nwankwoala, 2011. Aspects of the hydrogeology of Umuahia-South local government area, Abia State, Nigeria. J. Environ. Res. Manage., 2: 14-26.
25. Michael, J.F., E.R. Thomas, G.R. Michael and R.H. Dennis, 2005. Assessing groundwater vulnerability to contamination: Providing scientifically defensible information to decision makers. United States Geological Survey, USA.
26. Mercer, J.W. and C.R. Faust, 1980. Groundwater modelling: An overview. Groundwater, 18: 108-115.
27. Vrba, J. and A. Zaporozec, 1994. Guidebook on mapping groundwater vulnerability. International Association of Hydrogeologists, Verlag Heinz Heise GmbH & Co KG, Hanover, Germany.
28. Barbash, J.E. and E.A. Resek, 1996. Pesticides in Ground Water: Distribution, Trends and Governing Factors. Ann Arbor Press, Ann Arbor, Michigan,.
29. Bachmat, Y. and M. Collin, 1987. Mapping to Assess Groundwater Vulnerability to Pollution. In: Vulnerability of Soil and Groundwater to Pollutants, Van Duijvenbooden, W. and H.G. Van Waegeningh (Eds.)., TNO Committee on Hydrogeological Research, Hague, Netherlands, pp: 297-307.